Article

The Use of Cool Pavements for the Regeneration of Industrial Districts

Silvia Croce [1,2,*], Elisa D'Agnolo [2], Mauro Caini [2] and Rossana Paparella [2]

1 Institute for Renewable Energy, European Academy of Bozen/Bolzano (Eurac Research), Viale Druso 1, 39100 Bolzano, Italy

2 Department of Civil, Environmental and Architectural Engineering, University of Padova, Via Marzolo 9, 35131 Padova, Italy; elisa.dagnolo@unipd.it (E.D.); mauro.caini@unipd.it (M.C.); rossana.paparella@unipd.it (R.P.)

* Correspondence: silvia.croce@eurac.edu; Tel.: +39-0471-055-713

Abstract: Industrial districts are characterized by the presence of low and extensive building volumes and by predominantly sealed, impermeable surfaces, which contribute to several environmental problems and to the deterioration of outdoor human thermal comfort conditions, especially during summer hot days. To tackle these issues, this study proposes an approach for the regeneration of industrial districts based on the application of cool materials. Reflective and evaporative pavements were selected as suitable solutions to reduce summer overheating, while ensuring the functionality required by the industrial production, and contributing to stormwater management. The effectiveness of the approach was tested in a portion of the industrial district of Padua (Italy). In summer conditions, the replacement of conventional pavements with cool materials results in a reduction of the ground surface temperatures up to 14.0 °C and a consequent decrease of the air temperature at pedestrian level between 0.6 and 1.2 °C. The effects of human thermal comfort conditions highly depend on the selected cool material and on the morphology of the urban canyon. Finally, the reduction of external surface and air temperatures also contributes in cooling indoor spaces (average decrease from 1.0 to 2.5 °C), with impacts on the energy efficiency of the industrial buildings.

Keywords: urban regeneration; urban surfaces; cool materials; evaporative pavements; reflective pavements; urban microclimate; urban heat island; industrial districts

1. Introduction

The massive urbanization and the rapid growth of urban population worldwide, estimated to result in more than 6 billion inhabitants by 2050 [1], are accentuating various energy and environmental issues clearly related to anthropogenic causes. Several studies have demonstrated the link between urban development and climate change, and the unique climate risks, such as urban heat island and flooding, faced by urban areas [2,3]. At the urban scale, several adaptation and mitigation strategies are being proposed and implemented in central or residential areas [4–7]; however, less attention is being placed on industrial districts, despite that they occupy large proportions of built-up areas and are mainly characterized by impermeable surfaces. Indeed, the replacement of natural surfaces with artificial materials is responsible for the significant increase of air temperature in urban areas compared to the surrounding environment (i.e., urban heat island effect (UHI)), and land sealing, which in turn results in surface stormwater runoff problems [8]. Furthermore, the creation of new industrial districts intensifies land consumption, inducing relevant changes in the land use, including the reduction of green spaces, and consequential environmental impacts [9,10]. Despite their impacts and size, only a few previous studies focused on industrial areas, mainly assessing their contribution to UHI [11–14]. The present study analyses the main features and microclimatic conditions of an industrial district located in Padua (Italy), selected for its urban morphology, which is representative of the

majority of the European industrial districts. Furthermore, it proposes the application of cool materials as suitable regeneration strategy for the urban surfaces in industrial areas, and analyses the impact and benefits of such solutions on the microclimate and thermal comfort conditions.

1.1. Cool Materials for the Regeneration of Ground Surfaces: Techniques and Effects

The term cool materials defines all those materials or paintings able to maintain lower surface temperatures, compared to traditional ones, by absorbing and storing reduced quantities of solar radiation or by enhancing water evaporation [15]. Solutions for ground surfaces include (i) highly reflective and emissive, and (ii) evaporative pavements [16].

In this study, the focus was placed on the regeneration of conventional paving materials with cool ones for two major reasons. Firstly, intervening only on ground surfaces allows to maintain the functionality required by industrial production and to reduce the time needed for regeneration interventions. Secondly, a large fraction of urban areas—30% to 40%—is covered by pavements (e.g., roads, sidewalks, parking areas, etc.) [17]; hence, they significantly influence the local climate conditions, and the UHI development [18]. Previous studies have shown that the application of cool materials on ground surfaces contributes to a higher reduction of surface temperature—and consequently air temperature—than their application on building surfaces [19].

1.1.1. Reflective Pavements

The most popular cool materials are characterized by high solar reflectivity (i.e., ability of a material to reflect solar radiation) and high infrared emissivity (i.e., ability of a surface to release absorbed heat). These characteristics help to decrease the surface temperature, reducing the convection of heat from the pavement to the atmosphere and thereby decreasing the air temperature. Previous studies have demonstrated that an increased albedo by 0.1 is estimated to reduce the maximum pavement surface temperature by more than 3.0 °C [20,21]. Lower air temperatures contribute in mitigating the UHI effect [22], while also decreasing the energy demand for cooling, and slowing the formation of urban pollution [23]. Furthermore, an albedo increase at the urban scale can reduce the absorption of incoming solar radiation by the surface–troposphere system, contributing to counteract the global effects of the increase in greenhouse gas concentrations. Indeed, it has been estimated that increasing the pavement albedo by 0.15 in urban areas worldwide would reduce CO_2 emissions by 20 Gt [17]. Moreover, the lower temperatures reached by the pavements favor a greater durability of materials, extending their lifetime and reducing waste production from maintenance operations [24]. Finally, reflective pavements can improve visibility during night-time, leading to a potential reduction of lighting requirements and connected energy consumption [25].

Reflective materials were originally designed to be white or light colored and highly reflective in the visible wavelength. However, the increase of pavements solar reflectance can potentially result in glare problems, or in human thermal discomfort conditions in areas where people are exposed to the reflected radiation. In order to avoid these problems, successive scientific developments have led to materials that absorb in the visible part of the radiation spectrum, hence appearing to have a specific color, and are highly reflective in the near-infrared spectrum [26]. For applications on ground surfaces, reflective pavements include a wide range of materials and techniques, such as the use or white or light colored aggregates in asphalt or concrete mixes, resin-based pavements, and colored asphalt or concrete. In the case of urban regeneration, suitable solutions for existing ground surfaces include the use of reflective paints, resurfacing with chip seals, slurry seals, whitetopping, and microsurfacing with high albedo materials [27]. Table 1 presents an overview of the different technologies, their albedo values, and the surfaces where these can be applied.

Table 1. Technologies and solutions for the regeneration of existing ground surfaces with reflective materials. Application—solutions suitable (✔) for asphalt surfaces (A), and/or concrete pavements (CP).

Technology/Solution	Description	Albedo	Application A	CP	Ref.
Reflective paints	• Dark infrared reflective paint with hollow ceramic particles	0.50	✔	-	[28]
	• Near-infrared colored reflective paints	0.27–0.70	✔	✔	[29,30]
	• High-reflective white paint	0.80–0.90	-	✔	
Heat reflective paints	• Covering all aggregates	0.46–0.57	✔	-	[27,31]
	• Covering surface aggregates	0.25–0.60	✔	-	[27]
Chip seals	High-albedo aggregates bond in liquid asphalt. It is only used on roads with low traffic volumes, and is most effective when applied on large, exposed areas, such as parking lots.	0.29–0.44	✔	✔	[27,32]
Slurry seals	Mix containing asphalt emulsion, graded aggregate, additives, and water, acting as a hardwearing cover for the existing pavement. It is mainly suitable for low-volume traffic roads.	0.30–0.45	✔	✔	[27,32]
Whitetopping	Resurfacing of aged pavements by a layer—around 10 cm—of light colored Portland cement concrete, often containing fibers for added strength. Appropriate method for roads with medium to high traffic volumes, and parking lots, as it is characterized by elevated structural capacity and good grip, which favors road safety.	0.30–0.45	✔	✔	[15,27,33,34]
Microsurfacing	Rehabilitation technique that consists of a thin sealing layer of bituminous mixture. Light-colored materials can be used to increase the solar reflectance of asphalt. It provides a durable, highly skid-resistant surface, reduces maintenance costs, and increases the pavement life. Appropriate for roads with all conditions of vehicular traffic.	0.35–0.65	✔	-	[27,32,35]

1.1.2. Evaporative Pavements

Evaporative pavements are designed for holding water for evaporative cooling purposes (i.e., the use of latent heat emissions due to evaporation to reduce surface temperatures) and for avoiding stormwater runoff. These solutions are characterized by a higher amount of air voids than common pavements. The increased degree of air voids favors the infiltration of water both from the soil below and from the surface; therefore, part of the energy absorbed is diverted to water evaporation, reducing the heat emission [36]. As the evaporation process consumes energy, scientific literature reports that evaporative pavements help to reduce the surface temperature of the pavement up to about 20 °C compared to conventional ones [18,37–39]. A recent study from Vaillancourt et al. demonstrated that, if well-constructed and maintained, permeable pavements can reduce peak runoff flow rates and runoff volumes, and that this is true also when installed over poorly draining soils. Furthermore, infiltration rates are maintained during winter also in cold climates. Indeed, the air voids in the pavements insulate the sub-base and prevent it from freezing [40]. Other environmental benefits of evaporative pavements include (i) groundwater recharge, (ii) reduction of the discharge of pollutants, (iii) air quality improvement, and (iv) noise reduction on roads and highways [15,18,41].

Evaporative pavements include porous, permeable, pervious, and water-retaining solutions [15]. The characteristics and fields of application of each solution are detailed in Table 2.

Table 2. Technologies and solutions for evaporative pavements.

Technology/Solution	Description	Application	Ref.
Porous pavers	Present a higher porosity than conventional impermeable pavements. The presence of holes and connected pores allows water to flow through the material and to be stored when wet. The pavers generally present an interlocking structure, which can be filled with soil, gravel, or grass, the latter having the most significant cooling effect.	Non-road surfaces	[15,42]
Permeable pavements	Are constituted by concrete or clay bricks; the blocks themselves are impermeable but are disposed to leave small openings that allow water flow. Benefits include not only the mitigation of urban temperatures, but also the reduction of stormwater runoff, and the improvement of vehicles safety thanks to the increased friction properties.	Roads and non-roads surfaces	[15,43,44]
Pervious pavements	Special type of concrete pavements with high porosity level, which allow the flow of water. These include porous asphalt concrete, which can also be used on roads by laying a layer over the impermeable surface; this allows absorbing rainwater and diverting it to the side. Benefits encompass a cooling effect during dry periods, and road safety.	Roads and highways	[15,45]
Water-retentive pavements	Cement- or asphalt-based pavers in which the rainwater is kept in the layer close to their upper surface by water-retentive fillers.	Roads and non-road surfaces	[37,46–48]

2. Background

2.1. Geography and Climate of Padua

The city of Padua (45.41° N, 11.88° E) is located in the Veneto region, northern Italy, in a flat land (i.e., Po Valley) at an altitude of 12 m above sea level. Covering an area of around 93 km^2, with a population of 210,000 inhabitants (as of 2019) [49], Padua is the capital of the province and its economic and communications hub. The city is characterized by a climate in transition between humid subtropical and Mediterranean (Cfa and Csa/Csb according to the Köppen-Geiger classification [50]), with cold winters and hot summers (i.e., average air temperature (T_{air}) of 4.4 °C in January, and 25.2 °C in July) [51].

A recent analysis of climate change risks in Italy [52] estimated an increase in air temperature of up to 2 °C—which may reach 5 °C in the worst case scenario—in the period 2021–2050 compared to the period 1981–2010. Furthermore, it is expected an upsurge in the number of hot days and periods without rain, whereas intense precipitation events will also increase. In cities, the major amplifier of climate risk factors is the expected intensification of extreme climate phenomena, especially heat waves and intense rainfalls. In this context, the Veneto region is among the areas in Italy most affected by soil sealing, with

a share of more than 12% sealed surface [53] This results in several environmental issues, including the presence of urban heat island, and problems in stormwater management. A number of studies have confirmed the presence of UHI in Padua, especially during the summer seasons [51,54–56]. The UHI intensity is almost negligible during daytime, ranging from 0.4 to 0.8 °C, while during night-time is always higher than 4 °C, with peaks up to 9–10 °C [54–56]. The UHI results more intense in the historic center, where streets are characterized by high aspect ratio (i.e., ratio of the mean building height (H) to road width (W) (H/W)) and small sky view factor (i.e., portion of sky visible from a specific point inside the urban area (SVF)). It decreases in residential areas characterized by higher SVF, lower H/W ratio, and by the presence of green areas [54].

2.2. Case Study Area

The district selected as the case study is located in the ZIP, i.e., the industrial area of Padua. The ZIP, whose development started in 1946, is located in the eastern part of the city and is one of the largest industrial sites in Europe. It covers an area of over 11 km^2, corresponding to 8.5% of the total municipal area; as a comparison, the historical city center only covers around 5% (Figure 1a). It hosts more than 1300 industries, for a total of over 50,000 employees [4]. The ZIP presents the typical typical characteristics of Italian industrial areas developed between 1950 and 1970, with a regular urban geometry composed of large road axes for the transit of vehicles. It is characterized by a high proportion of land covered by buildings with large footprints, a wide presence of artificial materials, and a lack of vegetation. This results in high levels of soil sealing, with very few pervious surfaces. This is also confirmed by the mapping of the Biotope Area Factor Index, which expresses the share of ecologically effective area to total land area [57]. Nearly the entire industrial district is characterized by values equal to zero (i.e., totally impervious area) [53].
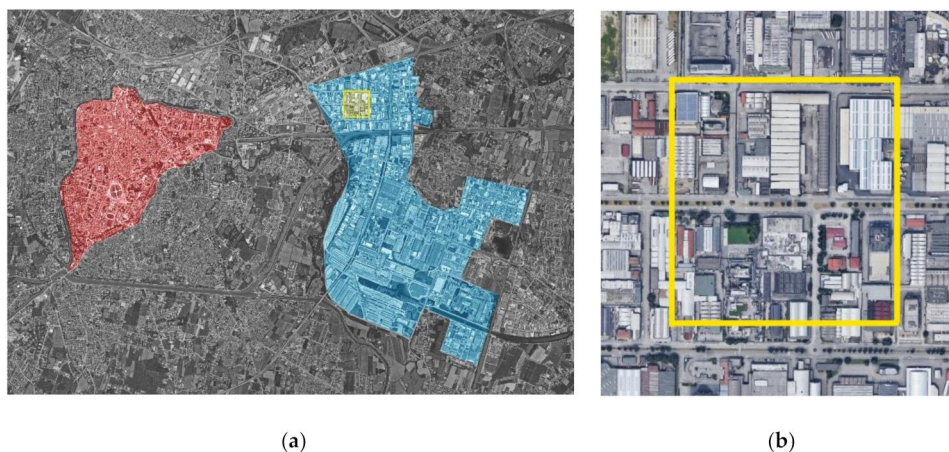

(a)   (b)

Figure 1. Aerial images. (**a**) Spatial relation between the historical city center (red) and the ZIP industrial district (blue); (**b**) case study area. The analyzed district is highlighted in yellow.

The study focused on a representative sector (Figure 1b), with the aim to evaluate the microclimatic impacts and potential benefits of the redevelopment of ground surfaces.

The analyzed area measures 380 × 400 m and is located in an area of the district not affected by boundary conditions, such as the cooling from the Piovego river at the west, or the anthropogenic heat released by the traffic on the motorway located to the east. Figure 2 shows the distribution of the typologies of urban surfaces in the selected district. Permeable surfaces are mainly associated with the presence of vegetated road dividers and small private green areas, corresponding to 6% of total horizontal surfaces. Buildings and their external service areas, together with the road network, cover the major share of the area; impermeable, artificial materials cover 94% of the horizontal surfaces. These characteristics

aggravate the risk of flooding in the event of intense rainfalls, and exacerbate the thermal stress in summer conditions.
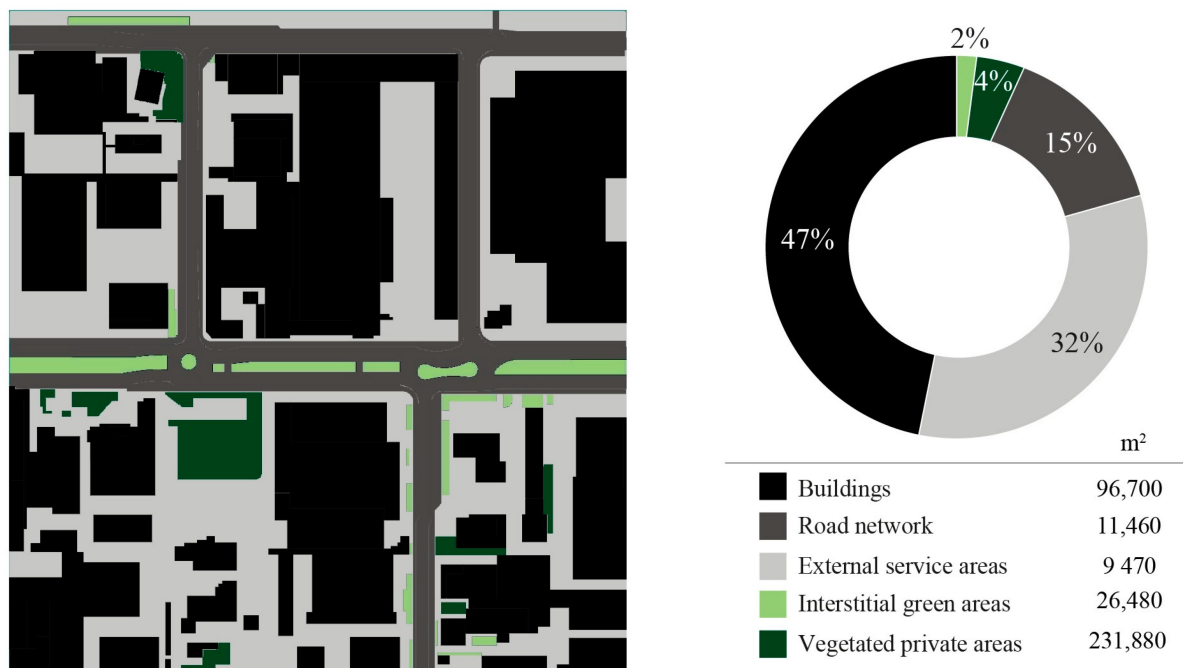

Figure 2. Share and extension of surface cover in the case study area.

3. Materials and Methods

3.1. Microclimate Analyses: Objectives, Inputs, and Tools

The microclimate analyses were focused on the following objectives:

1. identification of the major microclimate features of the industrial district in its current configuration;
2. assessment of the impacts and benefits of the application of cool materials on ground surfaces.

In order to accomplish these purposes, the numerical model ENVI-met, version 4.4, was used. ENVI-met is a 3D prognostic microclimate model able to simulate the surface–plant–air interactions in urban environments with a temporal resolution of 10 s and spatial resolution of 0.5–10 m [58]. The software physics is based on the calculation of both fluid dynamic characteristics, such as airflow and turbulence, and of thermodynamic and atmospheric processes [59]. ENVI-met allows one to (i) simulate the airflow around the structures and determine the complex micro-scale thermal interactions within urban environments; (ii) reproduce the diurnal cycle of the main climatic variables; (iii) calculate both the short-wave and long-wave radiation fluxes, and process the mean radiant temperature (T_{mrt}) for each cell of the model; and (iv) simulate the physical and physiological properties of vegetation [60,61]. In version 4, ENVI-met supports the simulation of complex vegetation geometries, through a three-dimensional vegetation module, and of water spray, including fountains. Furthermore, it allows one to "force" the climatic input parameters, defining their hourly values during the simulation period [59]. The simulations require two sets of input data: area input file and configuration file. The first contains the 3D model of the analyzed area, including the layout of the buildings, the materials of the surfaces, vegetation and soil types, and project location parameters. The latter include the settings for the initialization of the simulation, such as its start and duration, and the initial meteorological conditions.

3.2. Simulation Inputs

The 3D model of the examined block of the Padua industrial area was digitized with a resolution of 2 m in all directions, resulting in a model area of 190 × 200 cells in the x and y directions, respectively, and 30 cells in the z-direction. In order to reduce the influence of climatic boundary conditions at the borders of the model domain, a total number of six nesting grids with a coarser resolution was set at each the horizontal border [62]. The geometrical properties of the buildings (i.e., height, etc.), plants (i.e., type, height, volume, etc.) and ground (i.e., grass, asphalt, etc.) were checked using GIS data, aerial images, Google Maps 3D visualizations, and photos taken on-site. Thermo-physical and radiative properties of the urban surfaces were selected according to UNI 11300 [63] and ISO 10456-2007 [64]. The materials from the ENVI-met database were used for most common surfaces (e.g., asphalt, concrete, etc.), while the properties of cool pavements were collected from specific scientific literature, as detailed in Section 3.3.2.

The microclimate conditions were analyzed for the hottest day of summer 24 July 2019, which was selected as representative of typical hot conditions in Padua. The input climate data were collected from a weather station located in the industrial area, in *Corso Stati Uniti*, 2 km southeast of the case study area. These data were used in ENVI-met to "force" the model by providing the inflow boundaries for air temperature (T_{air}) and relative humidity (RH). The start of the simulations was set at 2:00 a.m., and the simulation time was 30 h, to observe the surface temperatures reached by the urban structure during the day and night until complete cooling (Table 3).

Table 3. Input data for the configuration of the ENVI-met model, and outputs of the analysis.

Start date and duration of simulation	Start date Total simulation time (h)	24 July at 02:00 30
Initial meteorological conditions	Wind speed (W_s) at 10 m height (m/s) Wind direction	2.20 West–South–West
Simple forcing setup	T_{air} (°C) RH (%)	$\min(T_{air\ @\ 7:00}) = 25.0$ $\max(T_{air\ @\ 18:00}) = 36.0$ $\min(RH_{@\ 18:00}) = 32$ $\max(RH_{@\ 7:00}) = 73$
Solar radiation and clouds	Adjustment factor for solar radiation Cover of medium clouds (octas)	1.00 2.00
Outputs of the analysis	Air temperature Relative humidity Wind speed Wind direction Short-wave solar radiation Mean radiant temperature Surface temperature	T_{air} (°C) RH (%) W_s (m/s) W_{dir} (°) Irr_{SW} (W/m^2) T_{mrt} (°C) T_s (°C)

3.3. Simulation Scenarios: Characterization of Urban Surfaces

The microclimate analyses were conducted in two scenarios: one representative of the current configuration of the area (i.e., Actual Scenario), and one accounting for a set of regeneration interventions with cool materials (i.e., Cool Pavements Scenario).

3.3.1. Actual Scenario

In the Actual Scenario (AS), the materials applied on the ground and building surfaces were maintained unvaried in order to characterize the current microclimate in the district.

The properties of buildings (i.e., height, materials, etc.), vegetation (i.e., type, height, etc.) and ground cover were selected based on aerial images and photos taken on-site. Thermo-physical properties were selected according to UNI 11300 [63] and ISO 10456-2007 [64], while the materials from the ENVI-met database were used for most common

surfaces (e.g., asphalt, concrete, etc.). With regard to ground surfaces (Table 4), the area is characterized by the diffused presence of impermeable materials with low albedo, i.e., asphalt and concrete. Vegetated areas, mainly grass surfaces and trees, were also included in the model.

Table 4. Properties of materials assigned to ground surfaces in the Actual Scenario.

Type of Pavement	Albedo	Emissivity	Volumetric Heat Capacity (J/mc K 10^{-6})	Thermal Conductivity (W/m K)	Ref.
Aged concrete	0.18	0.90	2.083	1.63	[42,65–68]
Aged asphalt	0.15	0.90	2.251	0.90	

Building surfaces present a higher variety of materials (Figure 3). Roofs materials include, among others, recently installed or aged black bituminous membranes, white EPDM (i.e., ethylene propylene diene monomer) membranes, metal roofing, and clay tiles. The façades are mostly constituted by concrete, and differ by the color of the plaster applied on them [69]. Table 5 presents the physical properties of the materials used to simulate the building surfaces in ENVI-met. To reduce the computational time, all the buildings were simplified in parallelepiped geometric shapes with flat roofs.
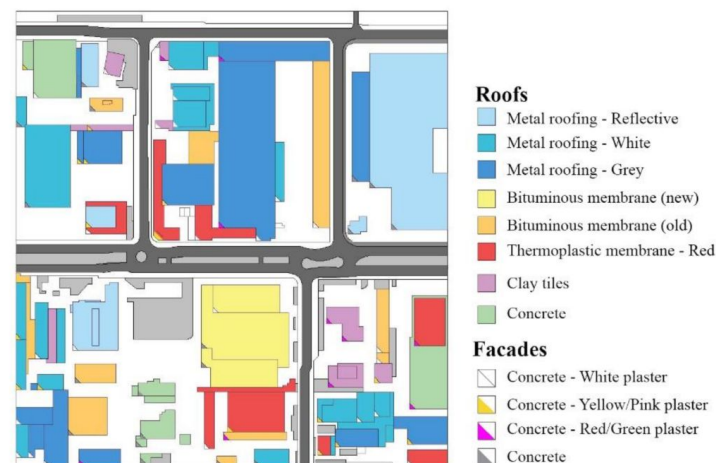

Figure 3. Materials assigned to building surfaces.

Table 5. Properties of materials assigned to building surfaces in both scenarios.

	Type of Material	Thickness (cm)	Albedo	Emissivity	Specific Heat (J/kg K)	Thermal Conduct. (W/m K)	Density (kg/mc)	Ref
Roofs	Bituminous membranes (new)	0.3	0.50	0.90	900	0.23	1200	[64,66,70–72]
	Bituminous membranes (aged)	0.3	0.15	0.90	900	0.23	1200	
	Thermoplastic membranes—red	0.3	0.40	0.90	900	0.23	1200	
	EPDM membranes	0.3	0.65	0.80	900	0.23	1200	
	Metal roofing—grey	2.0	0.40	0.10	4800	45.00	800	
	Metal roofing—white	2.0	0.60	0.10	4800	45.00	800	
	Metal roofing—reflective	2.0	0.80	0.10	4800	45.00	800	
	Clay tiles	5.0	0.55	0.90	840	0.70	2100	
	Concrete	3.0	0.30	0.90	840	1.30	2100	
Façades	White plaster	2.0	0.55	0.90	840	0.70	2100	[64–66,73]
	Yellow/Pink plaster	2.0	0.40	0.90	840	0.70	2100	
	Red/Green plaster	2.0	0.30	0.90	840	0.70	2100	

3.3.2. Cool Pavements Scenario

The Cool Pavement Scenario (CPS) analysed the impacts of the use of cool pavements for the regeneration of the district. The total regenerated ground surface had an extension of 73,200 m^2. Overall, the interventions proposed foresaw the application of reflective materials on 60,200 m^2, and the replacement of impermeable materials with permeable ones on 13,000 m^2. These interventions increased the share of permeable surfaces in the district to a total of 14%; this also contributes to the discharge of stormwater. Figure 4 shows the distribution of each ground material in the CPS scenario.
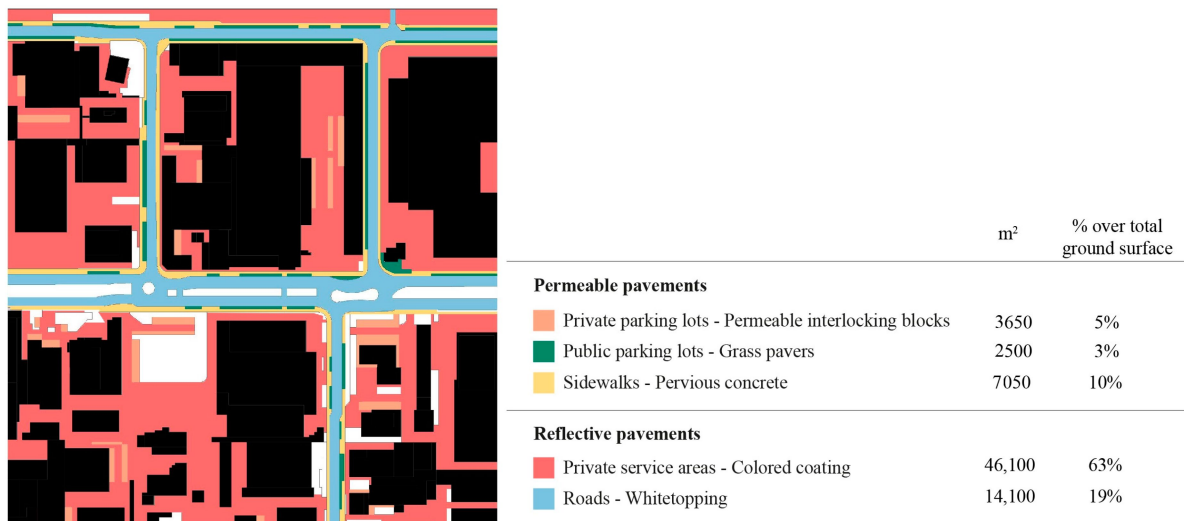

	m^2	% over total ground surface
Permeable pavements		
Private parking lots - Permeable interlocking blocks	3650	5%
Public parking lots - Grass pavers	2500	3%
Sidewalks - Pervious concrete	7050	10%
Reflective pavements		
Private service areas - Colored coating	46,100	63%
Roads - Whitetopping	14,100	19%

Figure 4. Materials assigned to ground surfaces in the Cool Pavements Scenario.

The properties of the materials selected for the regeneration of ground surfaces are presented in Table 6. Reflective materials were employed on roadways and private service areas. As these constitute the major share of ground surfaces, the choice was focused on solutions applicable on the existing materials. Although the replacement of asphalt and concrete might result in a more incisive intervention, it also entails environmental costs related to the disposal of waste. Moreover, in particular for the industry service areas, the application of the cool layer on top of the existing materials would reduce the time needed for the intervention, and consequently avoid the spaces being out of use for longer time. Whitetopping was selected for the application on roadways, as it presents a high resistance to heavy vehicular traffic, a good skid-resistance, and its albedo does not cause glare issues to drivers [33]. The material applied on the service areas of industries and companies consists of a colored asphalt coating layer. It presents a high durability of the reflective properties, high load-bearing capacity, and excellent mechanical strength [33,74].

Evaporative solutions were selected for parking areas and sidewalks to increase the share of permeable surfaces in the area. Indeed, in industrial areas, which are characterized by a high share of impermeable surfaces and require large asphalt service areas, the evaporative pavements can also serve for stormwater management, and for partially restoring the surface permeability for rainwater drainage, reducing damage and clogging of water systems during intense rainfall [45,75]. Private car parks were converted from impermeable asphalt to permeable interlocking concrete blocks. The sidewalks were designed in pervious concrete, a material suitable for light transit volumes and medium-to-low albedo, to ensure the visual comfort of users [15,45]. For the parking spaces alongside the roads, marked with parking lines on the asphalt, the use of grass paver grids was proposed to favor soil permeability and vegetation growth, both considered in the literature to be optimal mitigation systems [18,76]. The aim was to create a continuous belt capable of permeating rainwater in the subsoil, promoting the recharge of the aquifers, and resizing the water volumes to be discharged by the sewer system.

Table 6. Properties of materials assigned to ground surfaces in the Cool Pavements Scenario.

Type of Pavement	Albedo	Emissivity	Volumetric Heat Capacity (J/mc K 10^{-6})	Heat Conductivity (W/m K)	Ref.
Whitetopping	0.40	0.90	2.083	1.63	[34,64,68,77]
Pervious concrete	0.30	0.90	1.750	2.33	[15,64,78]
Colored asphalt	0.27	0.90	2.214	1.16	[64,79,80]
Permeable interlocking concrete blocks	0.50	0.90	2.000	2.00	[15,64]

3.4. Evaluation of Human Thermal Comfort Conditions

The thermal stress on the human body in the urban environment can be evaluated by integrating the environmental variables in the calculation of the equivalent temperature. This is defined as the ambient temperature of a reference environment that causes the same physiological response for a standard person as the actual one [81]. Several indexes have been developed for this purpose. This study selected the universal thermal climate index (UTCI) [82] for the evaluation of the effects of different ground surface materials on the urban thermal environment. The UTCI assesses the outdoor thermal environment for biometeorological applications [83,84], and it was selected as suitable as it provides a high level of detail with regard to human thermal responses in urban areas [85]. The calculation of UTCI depends on meteorological values, i.e., the actual values of air and mean radiant temperature, wind speed, and relative humidity, and non-meteorological values, i.e., metabolic rate and thermal properties of clothing. With regard to the latter, UTCI considers a reference person who walks at 4 km/h, generating a metabolic rate of 135 W/m^2 [82]. The value of UTCI identifies the thermal perception by human beings and the correlated grade of physiological stress. With relation to summer conditions, the range from 9 °C to 26 °C corresponds to "no thermal stress", from 26 °C to 32 °C to "moderate heat stress", and from 32 °C to 38 °C to "strong heat stress". UTCI values ranging from 38 °C to 46 °C describe a "very strong heat stress", and above 46 °C "extreme heat stress" conditions [86].

The ENVI-met's post-processing tool *BioMet* was used to calculate the UTCI, in compliance with the German standard VDI 3787-Part 2:2008 [87].

4. Results and Discussion

In this section, the relevant results related to the analyzed scenarios are discussed with regard to surface temperatures, air temperature and thermal comfort, and building indoor air temperature.
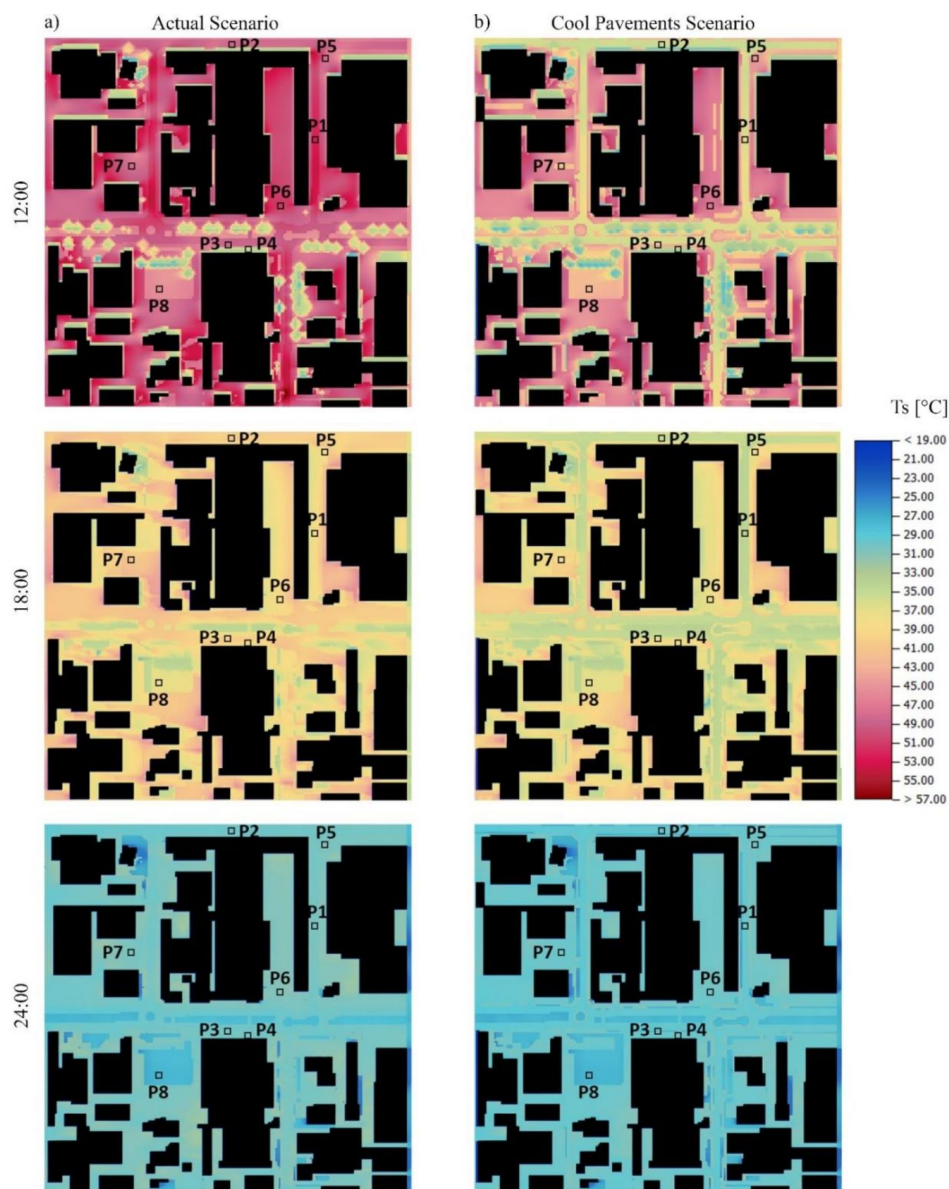
4.1. Surface Temperatures

The analysis of the surface temperatures in the two scenarios focused on both the ground and the building surfaces.

4.1.1. Ground Surfaces

The maximum ground surface temperatures (T_s) were reached at 12:00 of the reference day, 24 July 2019. In the Actual Scenario (AS in Table 7), asphalt temperatures were mostly uniform, varying from 47 to 53 °C, the higher values registered in urban canyons with the N–S axis. The vegetated areas exposed to the sun were about 10 °C cooler than the asphalt surfaces, while T_s in shaded areas ranged from 20 to 33 °C, both on asphalt surfaces shaded by trees, and on concrete surfaces shaded by buildings (Figure 5a), the latter values confirming the cooling effect provided by green surfaces, and natural or artificial shadings.

Table 7. Ground surface temperatures in AS, and absolute surface temperature difference between CPS and AS—24 July 2019.

Point	Ground Surface Cover		AS: T_s (°C)			CPS: ΔT_s (°C)		
	AS	CPS	12:00	18:00	24:00	12:00	18:00	24:00
P1	Aged asphalt (N–S)	Whitetopping	52.4	38.9	30.3	−14.8	−3.9	−0.5
P2	Aged asphalt (E–W, no trees)	Whitetopping	47.1	40.3	30.1	−12.2	−4.8	−0.4
P3	Aged asphalt (E–W, tree line)	Whitetopping	47.6	40.5	30.1	−11.4	−4.5	−0.7
P4	Aged asphalt	Pervious concrete	47.7	39.4	30.6	−2.9	−0.6	+0.2
P5	Aged asphalt	Grass pavers	47.7	39.5	30.5	−4.3	−3.4	−2.2
P6	Aged concrete	Colored asphalt	49.8	38.9	30.8	−2.3	−1.4	−0.9
P7	Aged concrete	Permeable interlock. concrete blocks	59.2	40.8	30.5	−5.7	−2.8	−0.6
P8	Grass	Grass	42.7	37.2	27.8	−0.5	−0.3	-

Figure 5. Development of ground surface temperatures in AS (**a**) and CPS (**b**) at different times of the analyzed day, 24 July 2019.

In the Cool Pavements Scenario (CPS in Table 7), the use of reflective and evaporative pavements produced an overall decrement of T_s in the entire case study area (Figure 5b). The highest reductions could be observed at 12:00 and varied depending on the solution adopted. The application of whitetopping over the existing road surfaces provided the most consistent cooling, with ΔT_s (i.e., absolute difference compared to the AS) ranging from 11.4 to 14.8 °C. Indeed, the surface temperature decreased from 52.4 °C (AS) to 37.6 °C (CPS) on the north–south urban canyons, while on the east–west ones, the reduction was lower, in both presence or absence of tree lines. The cool colored asphalt layer on the external private service areas produced a reduction of T_s up to 2.3 °C. The limited cooling effect, compared to the whitetopping surfaces, was related to the lower albedo (i.e., 0.27 compared to 0.40 of whitetopping). Pervious concrete had a moderate daytime benefit of −2.9 °C. The grass-paved areas had a lower albedo (i.e., 0.20), but produced a higher cooling effect, ranging from −4.3 °C to −3.4 °C during daytime. Indeed, the evapotranspiration processes due to the presence of vegetation provided a constant temperature reduction. Finally, the T_s of the already existing grass areas was also slightly reduced (i.e., ΔT_s ranging from −0.3 to −0.5 °C), demonstrating the capacity of surrounding materials to influence also the conditions of unmodified surfaces.

After the maximum at 12:00, the cooling benefits provided by the application of cool solutions gradually decreased (Table 7). At 18:00, the maximum cooling effect was less than –5.0 °C for all surfaces, and further reduced until midnight, when the minimum thermal benefits were provided (Figure 6). During night-time, whitetopping and colored asphalt were constantly cooler than conventional ground materials, thanks to the lower accumulation of daytime heat. On the contrary, T_s slightly increased on pervious concrete surfaces, ranging from +0.1 to +0.3 °C compared to AS. This demonstrates that reflection properties have greater influence during the daytime, while thermal properties are prevalent during the night-time [88,89]. The results are in line with previous studies, which confirmed the lower surface temperature of reflective materials compared to conventional materials [79,90].
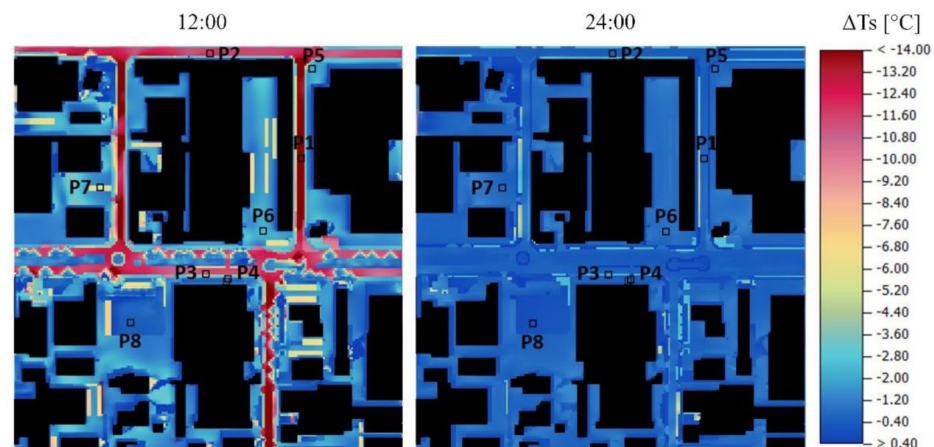

Figure 6. Absolute difference of ground surface temperature between CPS and AS at 12:00 and 24:00—24 July 2019.

4.1.2. Building Surfaces

The application of cool materials on ground surfaces also affects the T_s of building surfaces, due to the alterations in the radiative phenomena and the lowering of atmospheric temperature. The first effect is a variation of the facades' surface temperatures. In the Actual Scenario, T_s varied from 37.0 to 54.0 °C depending on the facades' characteristics, orientation, radiation conditions, and the type of surface in front of them. At 15:00, the hottest facades were those facing south. At this time, the temperature ranged from 40.0 to 41.0 °C on surfaces with white plaster, from 41.0 to 43.0 °C in the case of light colors, like yellow and pink, and from 43.0 to 45.0 °C in the case of darker colors and bare concrete.

During the afternoon, the highest T_s was registered on west facades. On these surfaces, temperatures were around 46.0 °C for the white color, 51.0 °C for the yellow–pink and red–green plasters, and 53–54.0 °C for the bare concrete. In the CPS, the increased albedo and consequent increased reflected radiation increased the facade T_s during the daytime (Figure 7). Dark surfaces, such as those with red/green plasters and concrete, were affected by an increase up to 0.6 °C compared to AS, mainly concentrated in the first meters from the ground. The increase was more noticeable on building surfaces facing canyons exposed to the direct solar radiation, i.e., south facades at 15:00, and west facades at 18:00.
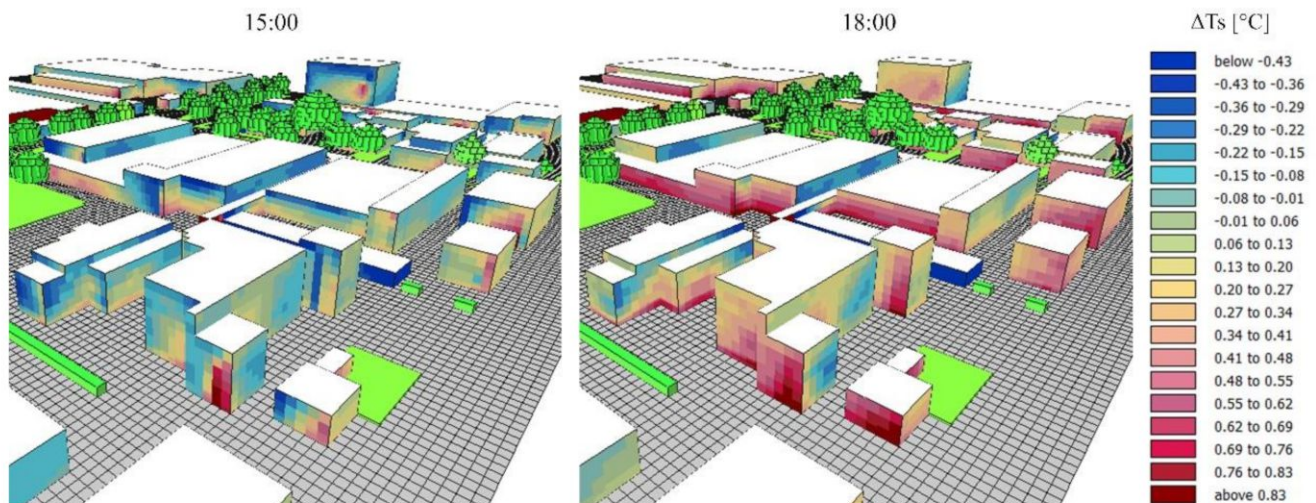

Figure 7. Absolute difference of building facades' surface temperatures between CPS and AS at 15:00 and 18:00—24 July 2019.

With regard to roof surface temperatures (Table 8), in the Actual Scenario, metal roofing presented lower temperatures than other roofing materials. Indeed, at 15:00, dark bituminous membranes reached the higher T_s, i.e., up to 76.5 °C, while light colored metal roofing surfaces were up to 27.0 °C cooler. This observation was validated in previous literature, which observed that light colored surfaces present lower surface temperatures during the daytime [22]. Conversely, at night, T_s was lower for clay tiles and concrete roofs, and higher for the metal surfaces. Indeed, the thermal conductivity of the bituminous membrane (i.e., 45 W/mK) favored a more rapid heat dispersion; on the contrary, steel (thermal conductivity of 0.23 W/mK) released the latent heat more gradually. The only exception was the reflective metal roofing, which—due to the higher albedo—presented lower T_s compared to other metal surfaces during both daytime and night.

In the Cool Pavements Scenario, the results highlighted a reduction of T_s, even though roofs materials were unchanged (Figure 8). At 15:00, the reduction of surface temperatures ranged from −1.3 to −10.1 °C; the greatest benefits were obtained at 18:00, when the reduction of external surface temperature was in a range from −2.2 to −17.9 °C. The smallest differences were recorded for the metal roofs, from −2.2 to −6.3 °C depending on the albedo. Concrete and roofing tiles had a T_s reduction of around −11.0 °C, while the bituminous membranes benefitted from a temperature decrease up to 17.5 °C. The replacement of current conventional pavements with cool materials generated a reduction of the air temperature in the district and, consequently, affected the roof surfaces.

Table 8. Surface temperatures of roofs in actual scenario (AS) and absolute difference between CPS and AS—24 July 2019.

Point	Roofing Material	AS—T_s ($^\circ$C)			CPS—ΔT_s ($^\circ$C)		
		15:00	**18:00**	**03:00**	**15:00**	**18:00**	**03:00**
R1	Bituminous membrane (new)	76.5	63.7	27.6	−10.1	−17.9	−0.8
R2	Bituminous membrane (aged)	74.6	62.6	27.4	−9.6	−17.1	−0.8
R3	Clay tiles	60.4	54.1	28.0	−6.7	−11.7	−0.9
R4	Concrete	59.4	53.9	29.9	−6.4	−11.3	−1.3
R5	EPDM membrane	48.9	44.1	26.6	−4.1	−7.2	−0.3
R6	Metal roofing—grey	44.6	46.2	34.8	−3.9	−6.3	−2.5
R7	Metal roofing—white	44.5	46.0	34.8	−3.8	−6.1	−2.2
R8	Metal roofing—reflective	32.1	33.4	29.3	−1.3	−2.2	−0.8
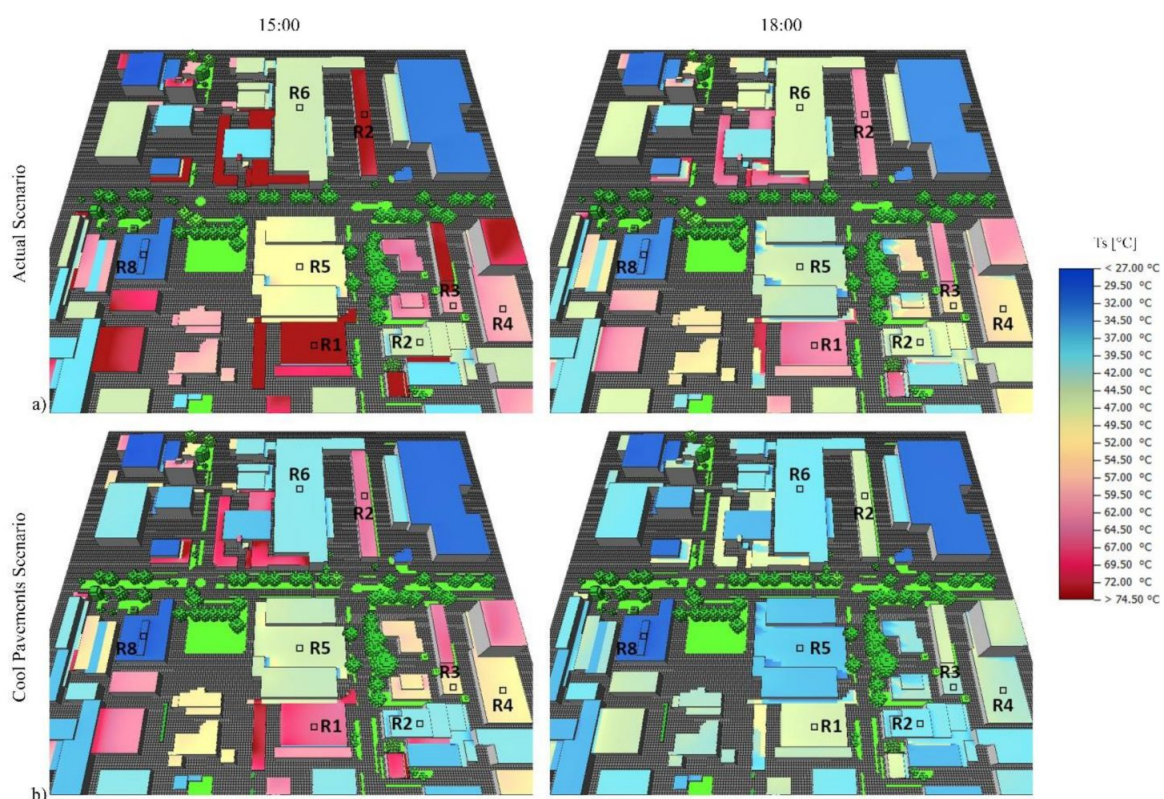
Figure 8. Surface temperature of buildings in AS (**a**) and CPS (**b**) at 15:00 and 18:00—24 July 2019.

4.2. Air Temperature

Microclimate analyses in the two scenarios also analyzed the air temperature at pedestrian level, showing a decrease in the comparison between Actual and Cool Pavement scenarios. The cooling effect was related to the reduction of surface temperatures, which in turn decreased the convection of heat from the ground to the air. At pedestrian level (i.e., 1.1 m a.g.l.), the maximum air temperature in both scenarios was registered at 15:00, with a delay of 3 h from the peak of the ground surface temperatures. The values were relatively uniform, in a range from 34.0 to 37.5 $^\circ$C in AS, and from 34.0 to 36.8 $^\circ$C in CPS. The cooler conditions were registered in proximity to grass surfaces and trees; in these locations, cool pavements did not provide a significant benefit. In CPS, areas with low SVF factor, such as narrow urban canyons, observed a moderate reduction of the air temperature up to 0.3 $^\circ$C. The decrement was more evident in canyons with east–west orientation and high SVF (ΔT_{air} from −0.6 to −1.2 $^\circ$C). The temperature gradient between the two scenarios

remained constant from 9:00 to 18:00; it afterwards decreased until 21:00 and remained unvaried around −0.2 °C during the night-time (Figure 9). These results were confirmed by previous studies, which reported a reduction of air temperature due to reflective pavements in the range between 0.15 and 3.0 °C [15,91].
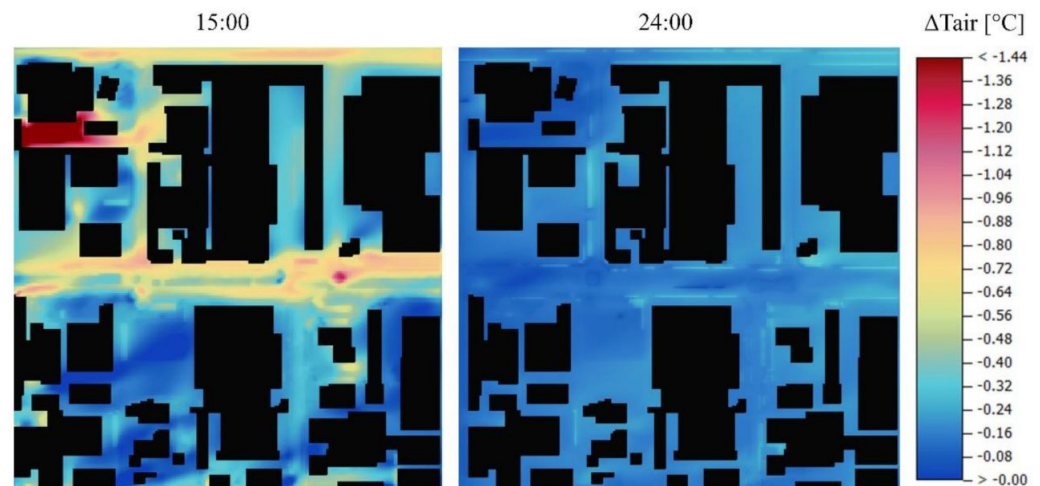

Figure 9. Air temperature absolute difference between CPS and AS at 15:00 and 24:00—24 July 2019.

The thermal benefits of cool materials were not limited to the pedestrian level. Indeed, they were also noticeable at higher levels from ground, as it was visible by analyzing the east–west section (Figure 10). In the AS, T_{air} was warmer near the buildings, up to an altitude of 20 m. The air temperature difference between the urban canopy layer and above was 2.0 °C in the morning, reached 3.5 °C at midday, and then it gradually decreased. From 21:00, no relevant differences could be observed. The CPS showed a reduction of T_{air} more intense at the building's quote, while the difference became negligible at an elevation above 30 m. At 10 m elevation, the reduction was up to 0.5 °C at 9:00, 0.6 °C at 12:00, and 0.2 °C at 21:00. At 30 m elevation, air temperature decreased up to 0.2 °C during daytime and 0.1 °C after sunset (i.e., 21:00).
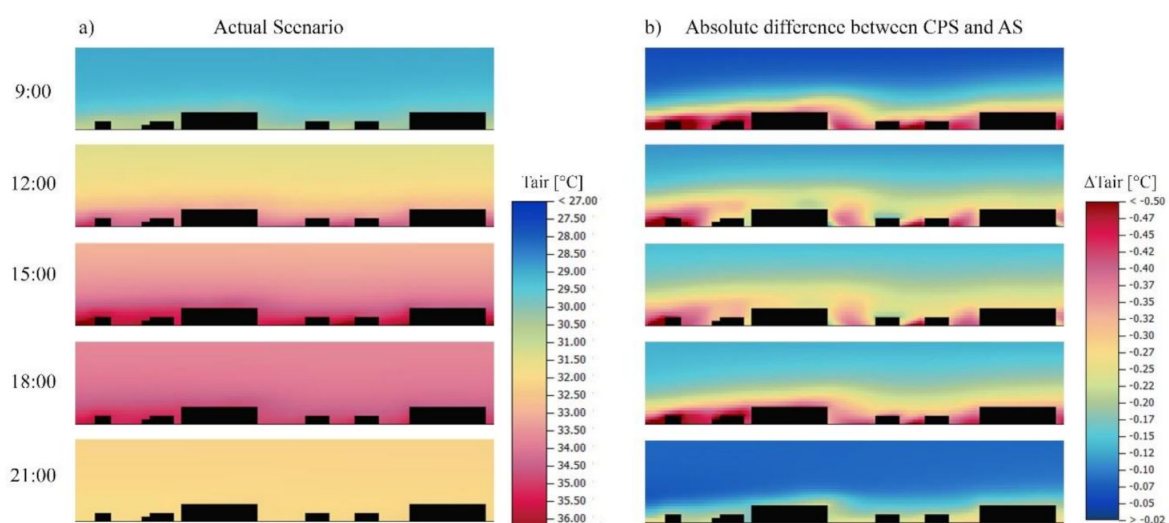

Figure 10. Air temperature in the E–W section of the district: actual Scenario (**a**) and absolute difference between CPS and AS (**b**)—24 July 2019.

4.3. Human Thermal Comfort

At pedestrian level, conditions of human thermal discomfort were perceived since the morning in both scenarios. In the Actual Scenario, at 8:00, the UTCI ranged from 33.4 to 37.0 °C in areas under direct solar radiation, corresponding to strong thermal stress; shaded areas record conditions of moderate thermal stress (i.e., UTCI values from 28.2 to 29.8 °C). At midday, the UTCI exceeded 40 °C, and it reached its maximum at 15:00 (Figure 11a), with very strong thermal stress conditions (i.e., UTCI from 44.2 to 46.6 °C), which endured until 17:00 m, when the temperature started to decrease.
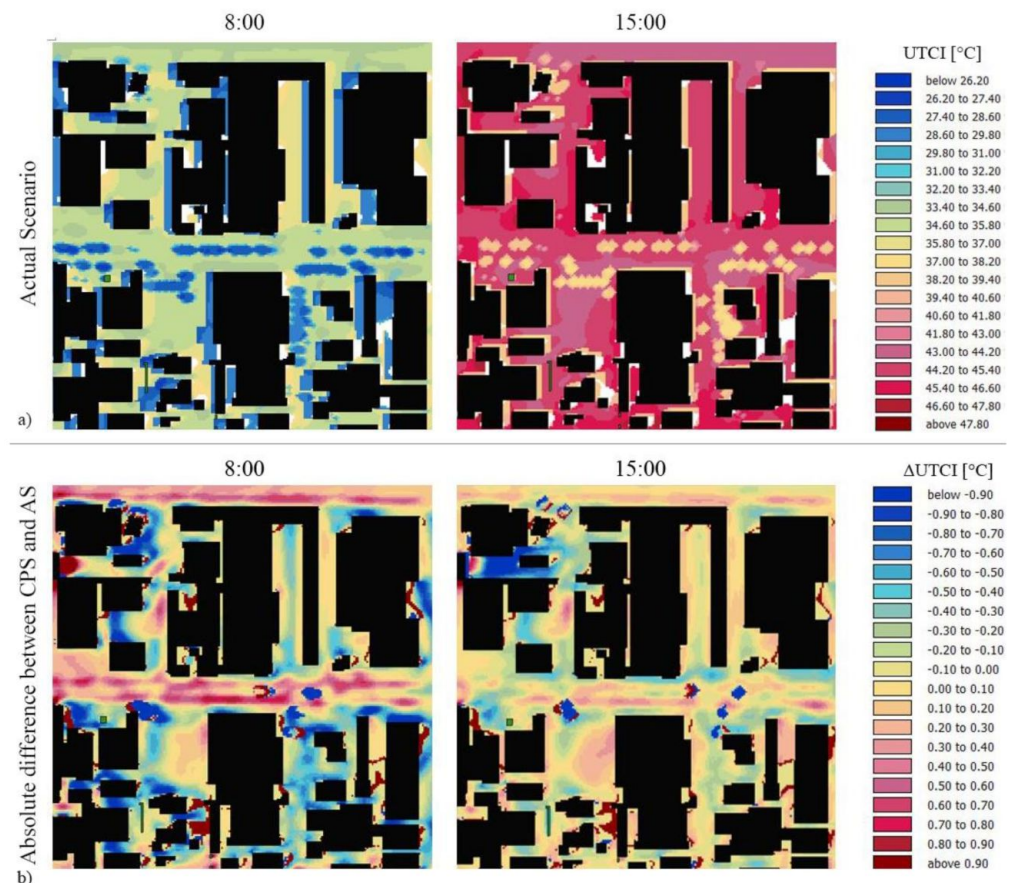

Figure 11. Thermal comfort conditions in the district at 8:00 and 15:00: UTCI in Actual Scenario (**a**), and absolute difference between CPS and AS (**b**)—24 July 2019.

The application of cool pavements did not change significantly the level of thermal stress during the daytime (Figure 11b). However, in the central hours of the day, the conditions of thermal stress were slightly worsened due to the increased pedestrian exposure to shortwave radiation reflected from pavements and walls, which also resulted in higher mean radiant temperatures. At 15:00, whitetopping (albedo = 0.45) increased the UTCI in the range 0.1 to 0.6 °C on east–west canyons, although the air temperature was 0.7 to 0.8 °C lower compared to AS at the pedestrian level. On the contrary, on southern fronts that overlooked tree-lined canyons, the shading and evapotranspiration of the vegetation provided a reduction of UTCI up to −0.3 °C. The colored asphalt applied on the service areas, with an albedo of 0.27, produced a reduction of UTCI up to 0.3 °C. The worsening of thermal comfort due to the application of reflective pavements under certain conditions, together with potential glare issues, were also confirmed in previous studies [34,92,93]. As a consequence, the design of regeneration interventions implying the use of reflective materials should place particular attention in the selection of the materials and their albedo to avoid these issues, especially in pedestrian areas [94]. The combined design of sidewalks

paved with reflective materials and shading canopies could generate thermal benefits for the users, particularly on the industries' external service areas.

With regard to evaporative pavements, permeable sidewalks and vegetated car parks were characterized by a constant reduction of UTCI compared to the AS (i.e., ΔUTCI from -0.1 to $-0.4\ ^\circ$C), thanks to the lower albedo and the evaporation of the humidity present in the cavities of the selected materials.

4.4. Effects on Buildings' Indoor Temperatures

The indoor temperatures of industrial buildings in the CPS were moderately cooler than the reference case (i.e., AS). Overall, the application of cool pavements led to a reduction of the indoor T_{air} in the layer immediately adjacent to the building envelope, as shown in Figure 12. In the CPS, the reduction of T_S on the building envelope entailed a decrease of indoor T_{air} up to 3 $^\circ$C. At 12:00, the reduction was moderate, from 0.6 to 0.7 $^\circ$C in buildings with metal roofing, and from -0.9 to $-1.8\ ^\circ$C for other types if roofs. The decrease was more evident during the afternoon, and reached its maximum at 18:00 (i.e., ΔT_{air} from -0.7 to $-1.5\ ^\circ$C for metal roofing, around $-1.5\ ^\circ$C for tiles, and around $-2.5\ ^\circ$C for dark and concrete roofs).
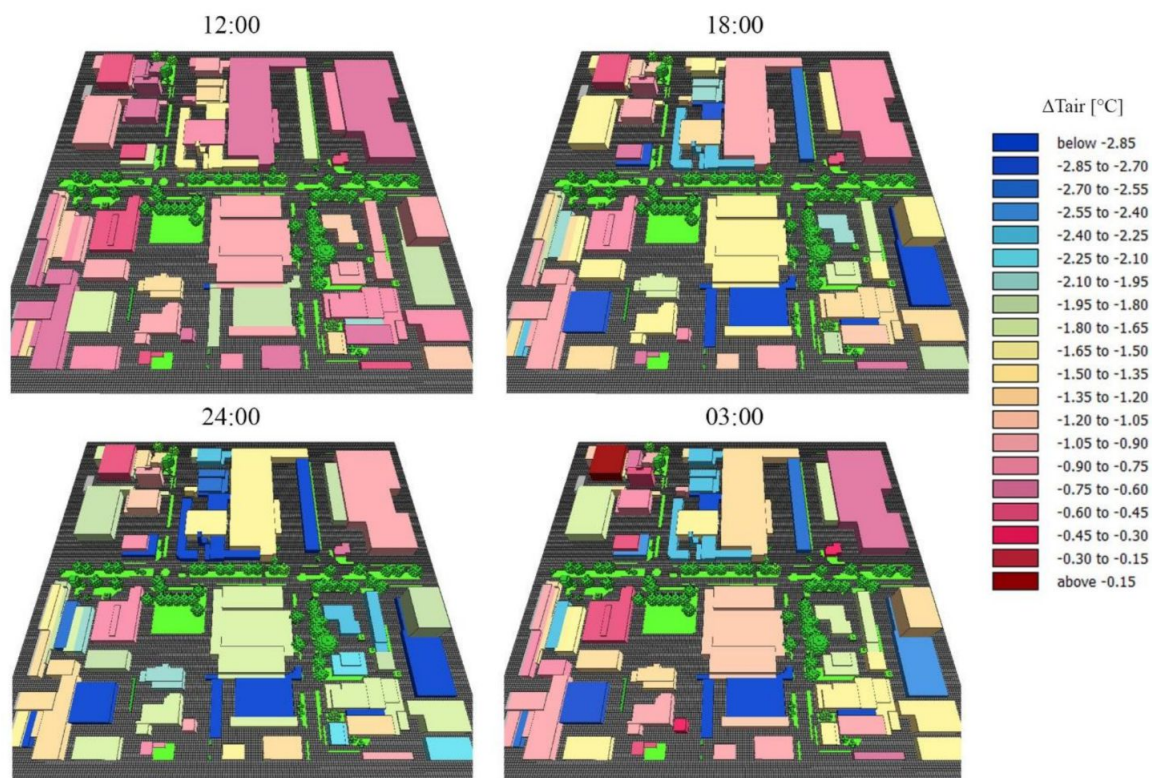

Figure 12. Cooling effect provided by the Cool Pavements Scenario inside the buildings: absolute air temperature difference compared to Actual Scenario—24 July 2019.

The indoor air temperature values in points distant from the external surfaces were not analyzed, and, consequently, the T_{air} reduction might be less marked. However, the analysis demonstrates that the use of cool pavements for the external ground surfaces might influence the thermal conditions inside buildings, leading to potential energy savings. This is confirmed by previous studies, which demonstrated that the energy consumption for cooling decreases as the albedo of city pavements increases [95–97], and that the application of cool materials might produce benefits in terms of indoor thermal comfort [98,99].

5. Limitations and Future Developments

This section presents some limitations of the study, together with its possible future developments.

In relation to the use of ENVI-met for microclimate analysis, some remarks on the results presented in this study are worth making. The model outputs strongly depend on the boundary conditions defined in the configuration file, which affect the simulation results. Previous studies have demonstrated that forcing these variables improves the accuracy of the outputs [19]. Therefore, a forcing setup was adopted for this study. However, the input climatic data were not collected directly on site, as this was not technically feasible, but from a weather station located at a distance of about 2 km southeast from the analyzed area. The selected weather station is located inside the ZIP, in an area with morphological characteristics similar to the one analyzed; nevertheless, this might affect the results. Furthermore, the lack of on-site monitored data did not allow the validation of the model. In previous validation studies, the ENVI-met model has demonstrated good approximations for T_{air} and T_s [19,100]. On the contrary, it has shown to overestimate T_{mrt} under shade and underestimate its values under long periods of sunlight; this can lead to inaccuracies in the calculation of human thermal comfort indexes, such as UTCI [19,101–105]. Some uncertainties should be considered in the analysis of the results.

- The model does not take into account the anthropogenic heat released from cooling systems and traffic [106]; this might lead to a potential underestimation of T_{air}.
- On the contrary, the model does not account for possible positive effects caused by local increments of wind speed at street level. Indeed, ENVI-met computes the W_S starting from the mean value measured at 10 m height, but the turbulence in a street canyon is normally higher than at higher levels [60,107], and hence might favor a local reduction of T_{air}.
- The model does not take into consideration the effect of multiple reflections and the consequent short- and long-wave radiation entrapment inside the urban canyons [19].
- Additionally, it is critical to consider the simplification related to the ENVI-met simulation of indoor air temperatures, which neglects heat from internal walls and anthropogenic sources such as computers, manufacturing machinery, and people [106].

In general, given the objective of the ENVI-met simulations in the present study (i.e., analysis of cooling effects of the regeneration of ground surfaces); the error resulting from daytime T_{air} underestimation is likely to retain the results on the conservative side.

Furthermore, cool pavements may provide environmental benefits, helping cities to meet their sustainability objectives; however, the replacement of materials and the change in pavement management practices can also impact upstream environmental burdens [108]. The second relevant limitation is related to the lack of estimation of the costs and life-cycle assessment of the proposed regeneration interventions.

The future developments of the study will focus on addressing all these limitations and expand the analysis at different scales.

- At the building scale, the indoor air temperature in points distant from the external surfaces should be analyzed to better quantify the impact of the regeneration of ground surfaces on indoor thermal comfort conditions and on building energy consumption for cooling.
- At the district scale, further simulations should be undertaken to investigate the effectiveness of other regeneration solutions (e.g., urban greening) or the combination of cool pavements with other technologies, also including their application on surfaces of the building envelopes. Furthermore, the analysis of the environmental conditions of the case study area in both scenarios should be extended to the entire summer period and other seasons, to expand the evaluation of the performance of cool paving solutions and to identify potential winter downsides. Another interesting aspect might be the estimation of the performance of cool pavements under future climatic

conditions in which the cooling and water infiltration capacities of such solutions might play an even more relevant role as mitigation strategies [109,110].

- At the urban scale, focus will be placed on the evaluation of the impacts of the regeneration interventions over a larger domain, as previous studies demonstrated that the effect of albedo increase is not restricted to the area of its application, but it also influences the air temperature of the surrounding areas [14].

6. Conclusions

The main purpose of the study was to analyze the effects of the replacement of conventional pavements with cool solutions as a regeneration intervention in industrial districts. A portion of the industrial area of Padua (Italy) was selected as a case study to carry out microclimate simulations. The results show that a combination of reflective and evaporative pavements can potentially help in decreasing urban surface temperatures, improving human thermal comfort conditions, mitigating urban heat island, and contributing to effective stormwater management. Indeed, during the hottest hours of a typical summer day (i.e., 29 July 2019), the replacement of conventional ground materials with reflective and evaporative pavements leads to the reduction of ground surfaces temperatures up to 14 °C and 6 °C, respectively. Accordingly, the air temperature at pedestrian level is also decreased, with ΔT_{air} values ranging from -0.6 up to -1.2 °C. The consequent effects of human thermal comfort conditions highly depend on the selected cool material and on the morphology of each urban canyon. In proximity to ground surfaces covered by whitetopping, UTCI is reduced up to 0.5 °C in shaded areas, while it increases up to 0.6 °C in areas directly exposed to sunlight, as a consequence of the increased reflected radiation. On the contrary, UTCI decreases up to 0.3 °C in service areas resurfaced with colored asphalt, and up to 0.4 °C in proximity to permeable pavements or green car parks. Benefits can also be observed in the indoor thermal conditions of industrial buildings, with a reduction of T_{air} in the layer immediately adjacent to the building envelope up to 2.5 °C. Therefore, the application of cool pavements in industrial districts can be a suitable intervention to reduce the summer energy consumption and the related greenhouse gas emissions, helping to limit global warming. Furthermore, in industrial areas characterized by a high share of impermeable surfaces and large asphalt service areas, the use of evaporative pavements can also serve for stormwater management, and for partially restoring the surface permeability for rainwater drainage.

Finally, the findings of the study can be summarized in some practical implications for the design of regeneration interventions with the use of cool pavements.

- The morphological configuration of the urban area plays a key role in the reduction of ground surface temperatures after implementing cool paving materials. Indeed, urban canyon orientation, aspect ratio, and sky view factor strongly affect the exposure of ground surfaces to direct solar radiation, and consequently impact the cooling potential of cool materials.
- At pedestrian level, the application of reflective pavements influences the radiative balance of the urban canyon surfaces and, consequently, the radiative exchange between the human body and the surrounding environment. Therefore, the achieved air temperature reduction might be counterbalanced by the increased reflection of solar radiation, negatively affecting the human thermal balance. On the contrary, the use of evaporative pavements produces limited, but constantly positive effects on the human thermal comfort. Hence, in the design of regeneration interventions with cool materials, particular attention should be placed on analyzing the impacts on thermal comfort conditions, and on avoiding their deterioration.
- The combination of reflective materials with trees and shading vegetation results in an effective solution for both cooling the air temperature and managing the increased reflected radiation due to the higher albedo. Indeed, the foliage not only contributes to release latent heat through evapotranspiration but also acts as shield for both direct and reflected solar radiation.

References

1. United Nations—Department of Economic and Social Affairs—Population Division. *World Urbanization Prospects: The 2018 Revision*; United Nations: New York, NY, USA, 2018.
2. Doherty, M.; Klima, K.; Hellmann, J.J. Environmental Science & Policy Climate Change in the Urban Environment: Advancing, Measuring and Achieving Resiliency. *Environ. Sci. Policy* **2016**, *66*, 310–313. [CrossRef]
3. Wang, C.; Wang, Z. Projecting Population Growth as a Dynamic Measure of Regional Urban Warming. *Sustain. Cities Soc.* **2017**, *32*, 357–365. [CrossRef]
4. Hirano, Y.; Ihara, T.; Gomi, K.; Fujita, T. Simulation-Based Evaluation of the Effect of Green Roofs in Office Building Districts on Mitigating the Urban Heat Island Effect and Reducing CO_2 Emissions. *Sustainability* **2019**, *11*, 2055. [CrossRef]
5. Zhang, M.; Bae, W.; Kim, J. The Effects of the Layouts of Vegetation and Wind Flow in an Apartment Housing Complex to Mitigate Outdoor Microclimate Air Temperature. *Sustainability* **2019**, *11*, 3081. [CrossRef]
6. Detommaso, M.; Gagliano, A.; Marletta, L.; Nocera, F. Sustainable Urban Greening and Cooling Strategies for Thermal Comfort at Pedestrian Level. *Sustainability* **2021**, *13*, 3138. [CrossRef]
7. Sen, S.; Roesler, J.; Ruddell, B.; Middel, A. Cool Pavement Strategies for Urban Heat Island Mitigation in Suburban Phoenix, Arizona. *Sustainability* **2019**, *11*, 4452. [CrossRef]
8. Tsoka, S.; Tsikaloudaki, K.; Theodosiou, T. Urban Space's Morphology and Microclimatic Analysis: A Study for a Typical Urban District in the Mediterranean City of Thessaloniki, Greece. *Energy Build.* **2017**, *156*, 96–108. [CrossRef]
9. Newman, P. The Environmental Impact of Cities. *Environ. Urban.* **2006**, *18*, 275–295. [CrossRef]
10. Parris, K.M.; Amati, M.; Bekessy, S.A.; Dagenais, D.; Fryd, O.; Hahs, A.K.; Hes, D.; Imberger, S.J.; Livesley, S.J.; Marshall, A.J.; et al. The Seven Lamps of Planning for Biodiversity in the City. *Cities* **2018**, *83*, 44–53. [CrossRef]
11. Mao, N. *Analysis of Urban Street Microclimate Data Based on ENVI-Met BT—Big Data Analytics for Cyber-Physical System in Smart City*; Atiquzzaman, M., Yen, N., Xu, Z., Eds.; Springer: Singapore, 2020; pp. 759–767.
12. Xiao, X.D.; Dong, L.; Yan, H.; Yang, N.; Xiong, Y. The Influence of the Spatial Characteristics of Urban Green Space on the Urban Heat Island Effect in Suzhou Industrial Park. *Sustain. Cities Soc.* **2018**, *40*, 428–439. [CrossRef]
13. El-Hattab, M.; Amany, S.M.; Lamia, G.E. Monitoring and Assessment of Urban Heat Islands over the Southern Region of Cairo Governorate, Egypt. *Egypt. J. Remote Sens. Sp. Sci.* **2018**, *21*, 311–323. [CrossRef]
14. Morini, E.; Touchaei, A.G.; Castellani, B.; Rossi, F.; Cotana, F. The Impact of Albedo Increase to Mitigate the Urban Heat Island in Terni (Italy) Using the WRF Model. *Sustainability* **2016**, *8*, 999. [CrossRef]
15. Qin, Y. A Review on the Development of Cool Pavements to Mitigate Urban Heat Island Effect. *Renew. Sustain. Energy Rev.* **2015**, *52*, 445–459. [CrossRef]
16. Tsoka, S.; Theodosiou, T.; Tsikaloudaki, K.; Flourentzou, F. Modeling the Performance of Cool Pavements and the Effect of Their Aging on Outdoor Surface and Air Temperatures. *Sustain. Cities Soc.* **2018**, *42*, 276–288. [CrossRef]
17. Akbari, H.; Matthews, H.D. Global Cooling Updates: Reflective Roofs and Pavements. *Energy Build.* **2012**, *55*, 2–6. [CrossRef]
18. Ferrari, A.; Kubilay, A.; Derome, D.; Carmeliet, J. The Use of Permeable and Reflective Pavements as a Potential Strategy for Urban Heat Island Mitigation. *Urban Clim.* **2020**, *31*, 100534. [CrossRef]
19. Tsoka, S.; Tsikaloudaki, A.; Theodosiou, T. Analyzing the ENVI-Met Microclimate Model's Performance and Assessing Cool Materials and Urban Vegetation Applications—A Review. *Sustain. Cities Soc.* **2018**, *43*, 55–76. [CrossRef]
20. Shimazaki, Y.; Aoki, M.; Nitta, J.; Okajima, H.; Yoshida, A. Experimental Determination of Pedestrian Thermal Comfort on Water-Retaining Pavement for UHI Adaptation Strategy. *Atmosphere* **2021**, *12*, 127. [CrossRef]
21. Chen, J.; Wang, H.; Zhu, H. Analytical Approach for Evaluating Temperature Field of Thermal Modified Asphalt Pavement and Urban Heat Island Effect. *Appl. Therm. Eng.* **2017**, *113*, 739–748. [CrossRef]
22. Doulos, L.; Santamouris, M.; Livada, I. Passive Cooling of Outdoor Urban Spaces. The Role of Materials. *Sol. Energy* **2004**, *77*, 231–249. [CrossRef]
23. Synnefa, A.; Karlessi, T.; Gaitani, N.; Santamouris, M.; Assimakopoulos, D.N.; Papakatsikas, C. Experimental Testing of Cool Colored Thin Layer Asphalt and Estimation of Its Potential to Improve the Urban Microclimate. *Build. Environ.* **2011**, *46*, 38–44. [CrossRef]
24. Li, H.; Harvey, J.T.; Holland, T.J.; Kayhanian, M. The Use of Reflective and Permeable Pavements as a Potential Practice for Heat Island Mitigation and Stormwater Management. *Environ. Res. Lett.* **2013**, *8*, 15023. [CrossRef]
25. Pomerantz, M.; Akbari, H.; Harvey, J.T. Cooler Reflective Pavements Give Benefits beyond Energy Savings: Durability and Illumination. *Proc. ACEEE Summer Study Energy Effic. Build.* **2000**, *8*, 789110.

26. Santamouris, M.; Synnefa, A.; Karlessi, T. Using Advanced Cool Materials in the Urban Built Environment to Mitigate Heat Islands and Improve Thermal Comfort Conditions. *Sol. Energy* **2011**, *85*, 3085–3102. [CrossRef]

27. Cheela, V.R.S.; John, M.; Biswas, W.; Sarker, P. Combating Urban Heat Island Effect—A Review of Reflective Pavements and Tree Shading Strategies. *Buildings* **2021**, *11*, 93. [CrossRef]

28. Kinouchi, T.; Yoshinaka, T.; Fukae, N.; Kanda, M. Development of Cool Pavement with Dark Colored High Albedo Coating. In Proceedings of the 5th Symposium on the Urban Environment, Vancouver, BC, Canada, 23–26 August 2004; pp. 207–210.

29. Karlessi, T.; Santamouris, M.; Apostolakis, K.; Synnefa, A.; Livada, I. Development and Testing of Thermochromic Coatings for Buildings and Urban Structures. *Sol. Energy* **2009**, *83*, 538–551. [CrossRef]

30. Hedayati, H.R.; Sabbagh Alvani, A.A.; Sameie, H.; Salimi, R.; Moosakhani, S.; Tabatabaee, F.; Amiri Zarandi, A. Synthesis and Characterization of Co1−xZnxCr2−yAlyO4 as a Near-Infrared Reflective Color Tunable Nano-Pigment. *Dyes Pigments* **2015**, *113*, 588–595. [CrossRef]

31. Boriboonsomsin, K.; Reza, F. Mix Design and Benefit Evaluation of High Solar Reflectance Concrete for Pavements. *Transp. Res. Rec.* **2007**, *2011*, 11–20. [CrossRef]

32. Tran, N.; Powell, B.; Marks, H.; West, R.; Kvasnak, A. Strategies for Design and Construction of High-Reflectance Asphalt Pavements. *Transp. Res. Rec.* **2009**, *2098*, 124–130. [CrossRef]

33. Krispel, S.; Peyerl, M.; Maier, G.; Weihs, P. Reduction of Urban Heat Islands with Whitetopping. *Bauphysik* **2017**, *39*, 33–40. [CrossRef]

34. Mizwar, I.K.; Napiah, M.; Sutanto, M.H. Thermal Properties of Cool Asphalt Concrete Containing Phase Change Material. *IOP Conf. Ser. Mater. Sci. Eng.* **2019**, *527*, 12049. [CrossRef]

35. Hein, D.; Olidis, C.; Darter, M.; Von Quintus, H. Impact of Recent Technology Advancements on Pavement Life. In Proceedings of the TAC/ATC 2003–2003 Annual Conference Exhibition Transport Assocation Canada Transport Factor, St. John's, Newfoundland and Labrador, Toronto, ON, Canada, 21–24 September 2003.

36. Hassn, A.; Chiarelli, A.; Dawson, A.; Garcia, A. Thermal Properties of Asphalt Pavements under Dry and Wet Conditions. *Mater. Des.* **2016**, *91*, 432–439. [CrossRef]

37. Higashiyama, H.; Sano, M.; Nakanishi, F.; Takahashi, O.; Tsukuma, S. Field Measurements of Road Surface Temperature of Several Asphalt Pavements with Temperature Rise Reducing Function. *Case Stud. Constr. Mater.* **2016**, *4*, 73–80. [CrossRef]

38. Takebayashi, H.; Moriyama, M. Study on Surface Heat Budget of Various Pavements for Urban Heat Island Mitigation. *Adv. Mater. Sci. Eng.* **2012**, *2012*, 523051. [CrossRef]

39. Nakayama, T.; Fujita, T. Cooling Effect of Water-Holding Pavements Made of New Materials on Water and Heat Budgets in Urban Areas. *Landsc. Urban Plan.* **2010**, *96*, 57–67. [CrossRef]

40. Catherine, V.; Sophie, D.; Geneviève, P. Hydrologic Performance of Permeable Pavement as an Adaptive Measure in Urban Areas: Case Studies near Montreal, Canada. *J. Hydrol. Eng.* **2019**, *24*, 5019020. [CrossRef]

41. Scholz, M.; Grabowiecki, P. Review of Permeable Pavement Systems. *Build. Environ.* **2007**, *42*, 3830–3836. [CrossRef]

42. Mohajerani, A.; Bakaric, J.; Jeffrey-Bailey, T. The Urban Heat Island Effect, Its Causes, and Mitigation, with Reference to the Thermal Properties of Asphalt Concrete. *J. Environ. Manag.* **2017**, *197*, 522–538. [CrossRef] [PubMed]

43. Stempihar, J.J.; Pourshams-Manzouri, T.; Kaloush, K.E.; Rodezno, M.C. Porous Asphalt Pavement Temperature Effects for Urban Heat Island Analysis. *Transp. Res. Rec.* **2012**, *2293*, 123–130. [CrossRef]

44. Li, H. *A Comparison of Thermal Performance of Different Pavement Materials*; Pacheco-Torgal, F., Labrincha, J.A., Cabeza, L.F., Granqvist, C.-G., Eds.; Woodhead Publishing: Oxford, UK, 2015; pp. 63–124. [CrossRef]

45. Li, H.; Harvey, J.; Ge, Z. Experimental Investigation on Evaporation Rate for Enhancing Evaporative Cooling Effect of Permeable Pavement Materials. *Constr. Build. Mater.* **2014**, *65*, 367–375. [CrossRef]

46. Bao, T.; Liu, Z.L.; Zhang, X.; He, Y. A Drainable Water-Retaining Paver Block for Runoff Reduction and Evaporation Cooling. *J. Clean. Prod.* **2019**, *228*, 418–424. [CrossRef]

47. Qin, Y.; He, Y.; Hiller, J.E.; Mei, G. A New Water-Retaining Paver Block for Reducing Runoff and Cooling Pavement. *J. Clean. Prod.* **2018**, *199*, 948–956. [CrossRef]

48. Jiang, W.; Sha, A.; Xiao, J.; Wang, Z.; Apeagyei, A. Experimental Study on Materials Composition Design and Mixture Performance of Water-Retentive Asphalt Concrete. *Constr. Build. Mater.* **2016**, *111*, 128–138. [CrossRef]

49. ISTAT. Population Data by Municipality. Available online: http://demo.istat.it/pop2019/index.html (accessed on 1 September 2020).

50. Kottek, M.; Grieser, J.; Beck, C.; Rudolf, B.; Rubel, F. World Map of the Köppen-Geiger Climate Classification Updated. *Meteorol. Z.* **2006**, *15*, 259–263. [CrossRef]

51. Noro, M.; Busato, F.; Lazzarin, R. UHI Effect in the City of Padua: Simulations and Mitigation Strategies Using the Rayman and Envimet Model. *Geogr. Pol.* **2014**, *87*, 517–530. [CrossRef]

52. Spano, D.; Mereu, V.; Bacciu, V.; Marras, S.; Trabucco, A.; Adinolf, M.; Barbato, G.; Bosello, F.; Breil, M.; Chiriacò, M.V.; et al. *Analisi Del Rischio. I Cambiamenti Climatici in Italia*; CMCC: Lecce, Italy, 2010. [CrossRef]

53. Pristeri, G.; Peroni, F.; Pappalardo, S.E.; Codato, D.; Castaldo, A.G.; Masi, A.; De Marchi, M. Mapping and Assessing Soil Sealing in Padua Municipality through Biotope Area Factor Index. *Sustainability* **2020**, *12*, 5167. [CrossRef]

54. Noro, M.; Lazzarin, R.; Busato, F. The Urban Corridor of Venice and The Case of Padua. In *Counteracting Urban Heat Island Effects in a Global Climate Change Scenario*; Musco, F., Ed.; Springer International Publishing: Cham, Switzerland, 2016; pp. 201–219. [CrossRef]

55. Noro, M.; Lazzarin, R. Urban Heat Island in Padua, Italy: Simulation Analysis and Mitigation Strategies. *Urban Clim.* **2015**, *14*, 187–196. [CrossRef]

56. Busato, F.; Lazzarin, R.M.; Noro, M. Three Years of Study of the Urban Heat Island in Padua: Experimental Results. *Sustain. Cities Soc.* **2014**, *10*, 251–258. [CrossRef]

57. Becker, G.; Mohren, R. *The Biotope Area Factor as an Ecological Parameter. Principles for Its Determination and Identification of the Target*; Landschaft Planen & Bauen: Berlin, Germany, 1990.

58. Bruse, M.; Fleer, H. Simulating Surface–Plant–Air Interactions inside Urban Environments with a Three Dimensional Numerical Model. *Environ. Model. Softw.* **1998**, *13*, 373–384. [CrossRef]

59. Bruse, M. ENVI-Met 4: A Microscale Urban Climate Model. 2015. Available online: www.envi-met.info (accessed on 20 January 2020).

60. Huttner, S. Further Development and Application of the 3D Microclimate Simulation ENVI-Met. Ph.D. Thesis, Universitätsbibliothek Mainz, Mainz, Germany, 2012.

61. Yang, X.; Zhao, L.; Bruse, M.; Meng, Q. Evaluation of a Microclimate Model for Predicting the Thermal Behavior of Different Ground Surfaces. *Build. Environ.* **2013**, *60*, 93–104. [CrossRef]

62. Lobaccaro, G.; Croce, S.; Vettorato, D.; Carlucci, S. A Holistic Approach to Assess the Exploitation of Renewable Energy Sources for Design Interventions Inthe Early Design Phases. *Energy Build.* **2018**, *175*, 235–256. [CrossRef]

63. CTI. UNI/TS 11300-Technical Standards Reference on Savings and Energy Certification of Buildings. 2016. (accessed on 1 February 2020).

64. ISO. ISO 10456:2007. Building Materials and Products: Hygrothermal Properties. Tabulated Design Values and Procedures for Determining Declared and Design Thermal Values. 2007. Available online: https://www.iso.org/standard/40966.html (accessed on 1 February 2020). [CrossRef]

65. Synnefa, A.; Santamouris, M.; Korres, D. Investigation of the Solar and Thermal Properties of Materials Used in Outdoor Urban Spaces and Buildings. In Proceedings of the 27th AIVC 4th Epic Conference Technologies Sustainable Policies a Radical Decrease Energy Consumption Building, Lyon, France, 20–22 November 2006.

66. Santamouris, M. *Environmental Design of Urban Buildings. An Integrated Approach*; Routledge: Oxfordshire, UK, 2019.

67. Levinson, R.; Akbari, H. *Effects of Composition and Exposure on the Solar Reflectance of Portland Cement Concrete*; Elsevier: Amsterdam, The Netherlands, 2002; Volume 32. [CrossRef]

68. Wang, Y.; Berardi, U.; Akbari, H. Comparing the Effects of Urban Heat Island Mitigation Strategies for Toronto, Canada. *Energy Build.* **2016**, *114*, 2–19. [CrossRef]

69. Lobaccaro, G.; Carlucci, S.; Croce, S.; Paparella, R.; Finocchiaro, L. Boosting Solar Accessibility and Potential of Urban Districts in the Nordic Climate: A Case Study in Trondheim. *Sol. Energy* **2017**, *149*, 347–369. [CrossRef]

70. Budaiwi, I.; Abdou, A. The Impact of Thermal Conductivity Change of Moist Fibrous Insulation on Energy Performance of Buildings under Hot-Humid Conditions. *Energy Build.* **2013**, *60*, 388–399. [CrossRef]

71. Santamouris, M.; Gaitani, N.; Spanou, A.; Saliari, M.; Giannopoulou, K.; Vasilakopoulou, K.; Kardomateas, T. Using Cool Paving Materials to Improve Microclimate of Urban Areas—Design Realization and Results of the Flisvos Project. *Build. Environ.* **2012**, *53*, 128–136. [CrossRef]

72. Prado, R.T.A.; Ferreira, F.L. Measurement of Albedo and Analysis of Its Influence the Surface Temperature of Building Roof Materials. *Energy Build.* **2005**, *37*, 295–300. [CrossRef]

73. Krimpalis, S.; Karamanis, D. A Novel Approach to Measuring the Solar Reflectance of Conventional and Innovative Building Components. *Energy Build.* **2015**, *97*, 137–145. [CrossRef]

74. Suksawang, N.; Alsabbagh, A.; Shaban, A.; Wtaife, S. Using Post-Cracking Strength to Determine Flexural Capacity of Ultra-Thin Whitetopping (UTW) Pavements. *Constr. Build. Mater.* **2020**, *240*, 117831. [CrossRef]

75. Thompson, A.M.; Kim, K.; Vandermuss, A.J. Thermal Characteristics of Stormwater Runoff from Asphalt and Sod Surfaces1. *JAWRA J. Am. Water Resour. Assoc.* **2008**, *44*, 1325–1336. [CrossRef]

76. Bartesaghi-Koc, C.; Haddad, S.; Pignatta, G.; Paolini, R.; Prasad, D.; Santamouris, M. Can Urban Heat Be Mitigated in a Single Urban Street? Monitoring, Strategies, and Performance Results from a Real Scale Redevelopment Project. *Sol. Energy* **2021**, *216*, 564–588. [CrossRef]

77. Satishkumar, C.H.N.; Siva Rama Krishna, U. Ultra-Thinwhite Topping Concrete Mix with Sustainable Concrete Materials—A Literature Review. *Int. J. Pavement Eng.* **2019**, *20*, 136–142. [CrossRef]

78. Sonebi, M.; Bassuoni, M.; Yahia, A. Pervious Concrete: Mix Design, Properties and Applications. *RILEM Tech. Lett.* **2016**, *1*, 109. [CrossRef]

79. Synnefa, A.; Santamouris, M.; Apostolakis, K. On the Development, Optical Properties and Thermal Performance of Cool Colored Coatings for the Urban Environment. *Sol. Energy* **2007**, *81*, 488–497. [CrossRef]

80. Rosso, F.; Golasi, I.; Castaldo, V.L.; Piselli, C.; Pisello, A.L.; Salata, F.; Ferrero, M.; Cotana, F.; de Lieto Vollaro, A. On the Impact of Innovative Materials on Outdoor Thermal Comfort of Pedestrians in Historical Urban Canyons. *Renew. Energy* **2018**, *118*, 825–839. [CrossRef]

81. Lai, D.; Liu, W.; Gan, T.; Liu, K.; Chen, Q. A Review of Mitigating Strategies to Improve the Thermal Environment and Thermal Comfort in Urban Outdoor Spaces. *Sci. Total Environ.* **2019**, *661*, 337–353. [CrossRef]

82. Bröde, P.; Fiala, D.; Blazejczyk, K. Calculating UTCI Equivalent Temperature. In Proceedings of the 13 th International Conference on Environmental Ergonomics, Boston, MA, USA, 2–7 August 2009; pp. 1–5.

83. Pappenberger, F.; Jendritzky, G.; Staiger, H.; Dutra, E.; Di Giuseppe, F.; Richardson, D.S.; Cloke, H.L. Global Forecasting of Thermal Health Hazards: The Skill of Probabilistic Predictions of the Universal Thermal Climate Index (UTCI). *Int. J. Biometeorol.* **2015**, *59*, 311–323. [CrossRef] [PubMed]

84. Jendritzky, G.; de Dear, R.; Havenith, G. UTCI—Why Another Thermal Index? *Int. J. Biometeorol.* **2012**, *56*, 421–428. [CrossRef]

85. Staiger, H.; Laschewski, G.; Matzarakis, A. Selection of Appropriate Thermal Indices for Applications in Human Biometeorological Studies. *Atmosphere* **2019**, *10*, 18. [CrossRef]

86. Park, S.; Tuller, S.E.; Jo, M. Application of Universal Thermal Climate Index (UTCI) for Microclimatic Analysis in Urban Thermal Environments. *Landsc. Urban Plan.* **2014**, *125*, 146–155. [CrossRef]

87. VDI. VDI 3787. Environmental Meteorology. Methods for the Human Biometeorological Evaluation of Climate and Air Quality for Urban and Regional Planning at Regional Level. Part I: Climate, Blatt 2/Part 2. 2008. Available online: https://infostore.saiglobal.com/en-us/standards/vdi-3787-2-2008-1116175_saig_vdi_vdi_2592309/ (accessed on 15 March 2020).

88. Wang, J.; Santamouris, M.; Meng, Q.; He, B.-J.; Zhang, L.; Zhang, Y. Predicting the Solar Evaporative Cooling Performance of Pervious Materials Based on Hygrothermal Properties. *Sol. Energy* **2019**, *191*, 311–322. [CrossRef]

89. Wang, J.; Meng, Q.; Zhang, L.; Zhang, Y.; He, B.J.; Zheng, S.; Santamouris, M. Impacts of the Water Absorption Capability on the Evaporative Cooling Effect of Pervious Paving Materials. *Build. Environ.* **2019**, *151*, 187–197. [CrossRef]

90. Taha, H. Urban Climates and Heat Islands: Albedo, Evapotranspiration, and Anthropogenic Heat. *Energy Build.* **1997**, *25*, 99–103. [CrossRef]

91. Yi, Y.; Jiang, Y.; Li, Q.; Deng, C.; Ji, X.; Xue, J. Development of Super Road Heat-Reflective Coating and Its Field Application. *Coatings* **2019**, *9*, 802. [CrossRef]

92. Lynn, B.H.; Carlson, T.N.; Rosenzweig, C.; Goldberg, R.; Druyan, L.; Cox, J.; Gaffin, S.; Parshall, L.; Civerolo, K. A Modification to the NOAH LSM to Simulate Heat Mitigation Strategies in the New York City Metropolitan Area. *J. Appl. Meteorol. Climatol.* **2009**, *48*, 199–216. [CrossRef]

93. Erell, E.; Pearlmutter, D.; Boneh, D. Effect of High-Albedo Materials on Pedestrian Thermal Comfort in Urban Canyons. In Proceedings of the ICUC8—8 th International Conference on Urban Climate, Dublin, Ireland, 6–10 August 2012; No. 8–11.

94. Pigliautile, I.; Pisello, A.L.; Bou-Zeid, E. Humans in the City: Representing Outdoor Thermal Comfort in Urban Canopy Models. *Renew. Sustain. Energy Rev.* **2020**, *133*, 110103. [CrossRef]

95. Bretz, S.; Akbari, H.; Rosenfeld, A. Practical Issues for Using Solar-Reflective Materials to Mitigate Urban Heat Islands. *Atmos. Environ.* **1998**, *32*, 95–101. [CrossRef]

96. Akbari, H.; Konopacki, S. Calculating Energy-Saving Potentials of Heat-Island Reduction Strategies. *Energy Policy* **2005**, *33*, 721–756. [CrossRef]

97. Dominnguez, S.; de la Flor, F.S. The Effect of Evaporative Techniques in Reducing Urban Heat. In *Urban Climate Mitigation Techniques*; Santamouris, M., Kolokotsa, D., Eds.; Routledge: London, UK, 2016.

98. Zinzi, M.; Fasano, G. Properties and Performance of Advanced Reflective Paints to Reduce the Cooling Loads in Buildings and Mitigate the Heat Island Effect in Urban Areas. *Int. J. Sustain. Energy* **2009**, *28*, 123–139. [CrossRef]

99. Castaldo, V.L.; Coccia, V.; Cotana, F.; Pignatta, G.; Pisello, A.L. Thermal-Energy Analysis of Natural "Cool" Stone Aggregates as Passive Cooling and Global Warming Mitigation Technique. *Urban Clim.* **2015**, *14*, 301–314. [CrossRef]

100. Acero, J.A.; Arrizabalaga, J. Evaluating the Performance of ENVI-Met Model in Diurnal Cycles for Different Meteorological Conditions. *Theor. Appl. Climatol.* **2018**, *131*, 455–469. [CrossRef]

101. Salata, F.; Golasi, I.; Petitti, D.; de Lieto Vollaro, E.; Coppi, M.; de Lieto Vollaro, A. Relating Microclimate, Human Thermal Comfort and Health during Heat Waves: An Analysis of Heat Island Mitigation Strategies through a Case Study in an Urban Outdoor Environment. *Sustain. Cities Soc.* **2017**, *30*, 79–96. [CrossRef]

102. Duarte, D.H.S.; Shinzato, P.; Gusson, C.d.S.; Alves, C.A. The Impact of Vegetation on Urban Microclimate to Counterbalance Built Density in a Subtropical Changing Climate. *Urban Clim.* **2015**, *14*, 224–239. [CrossRef]

103. Chow, W.T.L.; Brazel, A.J. Assessing Xeriscaping as a Sustainable Heat Island Mitigation Approach for a Desert City. *Build. Environ.* **2012**, *47*, 170–181. [CrossRef]

104. Jänicke, B.; Meier, F.; Hoelscher, M.-T.; Scherer, D. Evaluating the Effects of Façade Greening on Human Bioclimate in a Complex Urban Environment. *Adv. Meteorol.* **2015**, *2015*, 747259. [CrossRef]

105. Emmanuel, R.; Loconsole, A. Green Infrastructure as an Adaptation Approach to Tackling Urban Overheating in the Glasgow Clyde Valley Region, UK. *Landsc. Urban Plan.* **2015**, *138*, 71–86. [CrossRef]

106. Gros, A.; Bozonnet, E.; Inard, C. Cool Materials Impact at District Scale—Coupling Building Energy and Microclimate Models. *Sustain. Cities Soc.* **2014**, *13*, 254–266. [CrossRef]

107. Zölch, T.; Rahman, M.A.; Pfleiderer, E.; Wagner, G.; Pauleit, S. Designing Public Squares with Green Infrastructure to Optimize Human Thermal Comfort. *Build. Environ.* **2019**, *149*, 640–654. [CrossRef]

108. Gilbert, H.E.; Rosado, P.J.; Ban-Weiss, G.; Harvey, J.T.; Li, H.; Mandel, B.H.; Millstein, D.; Mohegh, A.; Saboori, A.; Levinson, R.M. Energy and Environmental Consequences of a Cool Pavement Campaign. *Energy Build.* **2017**, *157*, 53–77. [CrossRef]

109. Mauree, D.; Coccolo, S.; Perera, A.T.D.; Nik, V.; Scartezzini, J.L.; Naboni, E. A New Framework to Evaluate Urban Design Using Urban Microclimatic Modeling in Future Climatic Conditions. *Sustainability* **2018**, *10*, 1134. [CrossRef]
110. Naboni, E.; Natanian, J.; Brizzi, G.; Florio, P.; Chokhachian, A.; Galanos, T.; Rastogi, P. A Digital Workflow to Quantify Regenerative Urban Design in the Context of a Changing Climate. *Renew. Sustain. Energy Rev.* **2019**, *113*, 109255. [CrossRef]